A Dynamic Mean Field Theory for Dissipative Interacting Many-Electron Systems: Markovian Formalism and Its Implementation

SATOSHI YOKOJIMA,[1] GUANHUA CHEN,[1] RUIXUE XU,[2] YIJING YAN[2]
[1]*Department of Chemistry, The University of Hong Kong, Pokfulam Road, Hong Kong*
[2]*Department of Chemistry, Hong Kong University of Science and Technology, Kowloon, Hong Kong, and Open Laboratory of Bond-Selective Chemistry, University of Science and Technology of China, Hefei, People's Republic of China*

Received 6 February 2003; Accepted 6 May 2003

Abstract: To demonstrate its applicability for realistic open systems, we apply the dynamic mean field quantum dissipative theory to simulate the photo-induced excitation and nonradiative decay of an embedded butadiene molecule. The Markovian approximation is adopted to further reduce the computational time, and the resulting Markovian formulation assumes a variation of Lindblad's semigroup form, which is shown to be numerically stable. In the calculation, all 22 valence electrons in the butadiene molecule are taken as the system and treated explicitly while the nuclei of the molecules are taken as the immediate bath of the system. It is observed that (1) various excitations decay differently, which leads to different peak widths in the absorption spectra; and (2) the temperature dependences of nonradiative decay rates are distinct for various excitations, which can be explained by the different electron-phonon couplings.

 J Comput Chem 24: 2083–2092, 2003

Key words: QDT; TDHF; TDHF-QDT; Markovian; CS-QDT

Introduction

In a recent work,[1] we derived the time-dependent Hartree–Fock quantum dissipation theory (TDHF-QDT) and tested it on a two electron two-levels model system. The key entity in the TDHF-QDT is the reduced single-electron density matrix $\sigma(t)$, and thus, the numerical solution of TDHF-QDT is much more efficient than any existing quantum dissipation theories (QDTs). The reduced single-electron density matrix is defined by $\sigma_{jk} \equiv \langle c_k^\dagger c_j \rangle$ where $c_i^\dagger$ (c_i) is the creation (annihilation) operator of an electron on spin-orbital i. The equation of motion for $\sigma(t)$ derived in ref. 1 is given by

$$i\hbar\dot{\sigma} = [h, \sigma] - \frac{i}{\hbar}\sum_a [\eta_a, \sigma]\mathrm{tr}\{(\tilde{\eta}_a - \tilde{\eta}_a^\dagger)\sigma\} - \frac{i}{\hbar}\sum_a [\eta_a, (1-\sigma)\tilde{\eta}_a\sigma - \sigma\tilde{\eta}_a^\dagger(1-\sigma)] \quad (1)$$

where $h(t)$ is the time-dependent Fock matrix, and $\eta_a(t)$ and $\tilde{\eta}_a(t)$ are matrices related to the system-bath couplings, i.e.,

$$\eta_{a,jk}(t) = s_{jk}^a + \sum_{mn}(w_{jk,nm}^a - w_{jm,nk}^a)\sigma_{mn}(t), \quad (2)$$

$$\tilde{\eta}_a(t) = \sum_b \int_{-\infty}^{t} d\tau \tilde{C}_{ab}(t-\tau)\bar{G}(t,\tau)\eta_b(\tau)\bar{G}^\dagger(t,\tau). \quad (3)$$

Here, the system-bath interaction $\hat{H}_{SB}$ is assumed to be given by $\hat{H}_{SB} = -\sum_a \hat{W}_a\hat{F}_a$ with the Hermitian operator of the system $\hat{W}_a$

$$\hat{W}_a = \sum_{jk} s_{jk}^a c_j^\dagger c_k + \frac{1}{2}\sum_{jkk'j'} w_{jj',kk'}^a c_j^\dagger c_k^\dagger c_{k'} c_{j'}, \quad (4)$$

and the Hermitian operators in bath space $\hat{F}_a$, which can be considered as the generalized Langevin forces. $\tilde{C}_{ab}(t-\tau)$ and

Correspondence to: G. H. Chen; e-mail: ghc@everest.hku.hk; Y. J. Yan; e-mail: yan@chsg4.ust.hk

Contract/grant sponsors: Hong Kong Research Grant Council (RGC), the Committee for Research and Conference Grants of the University of Hong Kong, Research Grants of the Hong Kong University of Science and Technology, and the National Natural Science Foundation of China

$\bar{G}(t, \tau)$ are the bath correlation functions and the system Green's functions, respectively. As it was pointed out in ref. 1, it is expected that the TDHF-QDT can be used to simulate the nonradiative decays of realistic molecular systems. To demonstrate this, in this article we apply the TDHF-QDT to simulate the photoexcitation and subsequent nonradiative decay of a butadiene molecule. To integrate eq. (1) in time domain, we need to determine $\tilde{\eta}_a(t)$, which is computationally quite expensive. To simplify the computational complexity and reduce the computer time, we adopt the Markovian approximation and derive the Markovian version of TDHF-QDT formalism. The butadiene molecule is embedded in a liquid or solid environment. The system consists of all the valence electrons. The bath is made of two parts: the nuclei in the butadiene molecule constitute the immediate bath region and the liquid or solid surrounding the remote bath region. The immediate bath region has direct couplings to the system, and corresponds to $\hat{F}_a$ in the TDHF-QDT formalism. The remote bath region has no direct couplings to the system, and serves as the thermal sink for the immediate bath region that ensures the nuclei in the thermal equilibrium. H_S, H_{SB}, and H_B are either the first-principles Hamiltonians or the semiempirical models. It is important to emphasize that the resulting dissipation terms are derived from H_S, H_{SB}, and H_B by explicit integration over the bath degrees of freedom. Unlike most existing QDTs, these dissipation terms are therefore not phenomenological.

The objectives of this work are: (1) to demonstrate that TDHF-QDT approach can indeed be applied to realistic molecular systems and capture the essential physics of their energy dissipation processes; and (2) to examine the nonradiative decaying processes of an embedded butadiene molecule upon a photoexcitation, assuming the memory of the bath's dynamics is very short. The Markovian version of the TDHF-QDT is derived in the next section, and comparison to Lindblad semigroup formalism is discussed. Then, we apply our theory to simulate the photoexcitation and subsequent nonradiative relaxation of the embedded butadiene molecule at different temperatures. To interpret the simulation results, we explicitly evaluate the couplings between the electronic excitations and the vibrational modes. Discussion on the formalism and its future extension are given in the Discussion.

Markovian Approximation Versus Semigroup Formulation

The CS-QDT based TDHF formulation, eqs. (1) and (3), which is valid for arbitrary non-Markovian excitation-dissipation many-electron systems, is an integro-differential equation. The integral equation eq. (3) for $\tilde{\eta}_a(t)$ may be solved in a variety of ways such as the spectral density parameterization.[2,3] In ref. 1 an iterative algorithm is adopted, which is time consuming. When the Markovian approximation is employed, the numerical implementation of the TDHF-QDT can be greatly facilitated. The Markovian theory can be obtained via the white-noise ansatz under the standard Redfield approximation for eq. (3) (see ref. 1).

$$\tilde{\eta}_a(t) \approx \frac{1}{2} \sum_b C_{ab}(0)\, \eta_b(t), \tag{5}$$

where $C_{ab}(0)$ is the interaction spectrum $C_{ab}(\omega)$ taken at $\omega = 0$. From the detailed-balance relation, $C^*_{ab}(\omega) = e^{\beta\omega} C_{ab}(-\omega)$, we conclude immediately that $C_{ab}(0)$ is real; thus, $\tilde{\eta}_a$ under the Markovian approximation [eq. (5)] is Hermitian. As a result, eq. (1) reduces to

$$i\hbar\dot{\sigma} = [h, \sigma] - \frac{i}{2\hbar} \sum_{a,b} C_{ab}(0)[\eta_a, [\eta_b, \sigma]]. \tag{6}$$

This equation has the similar form as the Lindblad's dynamical semigroup construction.[4] To calculate $C_{ab}(0)$, we assume that $\tilde{C}_{ab}(t)$ decays exponentially

$$\tilde{C}_{ab}(t) \approx \tilde{C}_{ab}(0) e^{-|t|/\delta\tau} \tag{7}$$

where $\delta\tau \ll 1$ is a time-scale parameter that needs to be determined. Equation (7) leads to

$$C_{ab}(0) \approx 2\delta\tau \tilde{C}_{ab}(0) = 2\delta\tau\, \mathrm{Tr}_B[\hat{F}_a(0)\hat{F}_b(0)\rho_B^{eq}]. \tag{8}$$

To compare eq. (6) with the dynamical semigroup QDT,[4] we shall use the property of spectral functions that the matrix $\{C_{ab}(\omega)\}$ is positively defined (cf. Appendix B of ref. 1). We can thus define a Fock-space Hermitian matrix, K^ν, via its elements as

$$K^\nu_{jk} = \sum_a \eta_{a,jk} \sqrt{\Omega_\nu}\, D^\nu_a, \tag{9}$$

where $\{D^\nu_a\}$ and $2\Omega_\nu \geq 0$ being the ν^{th} eigenvector and eigenvalue of the matrix $\{\tilde{C}_{ab}(0)\}$. We can then recast eq. (6) in the following Lindblad-like form,

$$i\hbar\dot{\sigma} = [h, \sigma] - \frac{i}{\hbar}\, \delta\tau \sum_\nu [K^\nu, [K^\nu, \sigma]]. \tag{10}$$

Here, $\delta\tau$ is the characteristic time scale for the bath correlation function, and will be specified later [cf. eq. (7)]. The above equation differs from the conventional Lindblad's semigroup QDT, as both h and K^ν here are Fock-space matrices that depend on σ at local time. In the case where the two-electron components of the bath interaction can be neglected [i.e., $w^a_{jj',kk'} = 0$ in eq. (2)], K^ν becomes independent of σ, and therefore, the second term in eq. (10) does assume the Lindblad dissipation form. Note that although the dissipative term in eq. (10) is of Lindblad-like form, it has very different physical meanings. Equation (10) is the EOM for the reduced single-electron density matrix σ not the system density matrix ρ. The dynamical semigroup form of the nonlinear EOM for single-electron reduced density matrix is yet to be explored.

In the following, we shall consider the weak excitation regime in which it is sensible to linearize eq. (10). Denote $\sigma(t)$ as

$$\sigma(t) = \sigma^{(0)} + \delta\sigma(t), \tag{11}$$

where $\sigma^{(0)}$ is the equilibrium reduced single-electron density matrix, which is approximated by the ground state reduced single-electron density matrix in this work, and $\delta\sigma$ is the deviation or fluctuation that can be treated as small perturbation. To the first-order in $\delta\sigma$, eq. (10) becomes

$$i\hbar \frac{d}{dt} \delta\sigma = [h^{(0)}, \delta\sigma] + [\delta h, \sigma^{(0)}] - \frac{i}{\hbar} \delta\tau \sum_{\nu} [K^{\nu}, [K^{\nu}, \delta\sigma]], \tag{12}$$

where $h^{(0)}$ is the ground state Fock matrix, i.e.,

$$h_{jk}^{(0)} = t_{jk} + \sum_{mn} (v_{jk,nm} - v_{jm,nk}) \sigma_{mn}^{(0)}, \tag{13}$$

and

$$\delta h_{jk}(t) = f_{jk}(t) + \sum_{mn} (v_{jk,nm} - v_{jm,nk}) \delta\sigma_{mn}(t). \tag{14}$$

Here, we assume the system Hamiltonian is given by

$$\hat{H}_S(t) = \sum_{ij} t_{ij} c_i^{\dagger} c_j + \frac{1}{2} \sum_{jkk'j'} v_{jj',kk'} c_j^{\dagger} c_k^{\dagger} c_{k'} c_{j'} - \vec{E}(t) \cdot \sum_{ij} \vec{\mu}_{i,j}(t) c_i^{\dagger} c_j, \tag{15}$$

where t_{ij} and $v_{jj',kk'}$ are for the hopping terms and the electron–electron Coulomb integrals, respectively. The third term in eq. (15) is for the interaction between the system and the external electric field $\vec{E}(t)$, and $\vec{\mu}_{ij}$ is the dipole matrix element. We further define $f_{ij}(t) \equiv -\vec{E}(t) \cdot \vec{\mu}_{ij}$.

It is important that the integration of eq. (12) in the time-domain is stable. In Appendix A, we show that $\delta\sigma(t) \to 0$ globally as $t \to \infty$. This ensures that integrating eq. (12) is numerically stable. Equation (10) is a special case of the TDHF-QDT equation (1) when the Markovian bath is taken, and eq. (12) is the linear response version of eq. (10). Note that eq. (10) does not lead to the Fermi–Dirac distribution as $t \to \infty$ because the Markovian bath is adopted.

Excitation and Relaxation of a Butadiene Molecule

To demonstrate of the feasibility of applying the TDHF-QDT formalism to realistic complex molecular systems, we employ eq. (12) to simulate the photoexcitation and subsequent nonradiative relaxation of an embedded butadiene molecule in a liquid or solid matrix. The PM3 Hamiltonian[5] is used for $\hat{H}_S$. We denote the position of the atom by q_{ms} where the subscript s is for the direction. Then q_{ms} can be expanded as

$$q_{ms} = q_{ms}^{(0)} + \delta q_{ms}, \tag{16}$$

where $q_{ms}^{(0)}$ is q_{ms} in equilibrium and δq_{ms} is the deviation. The nuclei are taken as a part of the bath and couple directly to the valence electrons. The liquid or solid surrounding serves as an energy sink that ensures the nuclei in thermal equilibrium at a temperature T. The bath Hamiltonian $\hat{H}_B$ describes the vibration of these nuclei,

$$\hat{H}_B = \sum_{m,s} \frac{p_{ms}^2}{2M_m} + \frac{1}{2} \sum_{m,n,s,t} V_{ms,nt} \delta q_{ms} \delta q_{nt}, \tag{17}$$

where p_{ms} is the momentum component of the m-th atom along s-direction, $V_{ms,nt}$ is the effective interaction between two atoms m and n, and M_m is the mass of m-th atom. $\hat{H}_B$ can be determined directly from the vibrational modes and vibrational frequencies of these nuclei, and can thus be evaluated from the first principles or semiempirical calculations.

The system-bath coupling term H_{SB} describes the energetics when the nuclei deviate from their equilibrium positions. In the present work, we consider only the weak system-bath coupling case, i.e., $\hat{H}_{SB}$ is given by

$$\hat{H}_{SB} = \sum_{m,s} \frac{\partial \hat{H}_S}{\partial q_{ms}} \delta q_{ms}. \tag{18}$$

$\partial \hat{H}_S / \partial q_{ms}$ and δq_{ms} correspond to $\hat{W}_a$ and $\hat{F}_a$, respectively. δq_{ms} is relatively small, and $\hat{H}_{SB}$ is thus weak compared to $\hat{H}_S$ and $\hat{H}_B$. It is observed that the derivatives of t_{ij} with respect to q_{ms} are much larger than those of $v_{ij,kl}$, and we thus keep only $\partial t_{ij}/\partial q$ in the evaluation of $\partial h/\partial q$ in our calculations. In other words, the two-electron terms in $\partial \hat{H}_S / \partial q_{ms}$ are neglected. We have thus that $\eta_{a,ms} = s_{ms}^a = \partial t_{ij}/\partial q_{ms}$ and $\hat{F} = \vec{q}$. According to eq. (8),

$$\tilde{C}_{ab}(0) = Tr_B[q_a q_b \rho_B^{eq}]. \tag{19}$$

Utilizing the fact that the nuclei are in thermal equilibrium at T, we have

$$K_{ij}^{\nu} \equiv \sum_{m,s} \frac{\partial t_{ij}}{\partial q_{ms}} \sqrt{\frac{\hbar}{2M_m\omega_{\nu}} \coth\left(\frac{\beta\hbar\omega_{\nu}}{2}\right)} Q_{ms}^{\nu}, \tag{20}$$

where ω_{ν} and Q_{ms}^{ν} are the frequency and the m-th atom's displacement along the s-direction for the ν-th nuclear vibrational mode, respectively. In the derivation the nuclear–nuclear correlation $\langle \delta q_{m_1 s_1} \delta q_{m_2 s_2} \rangle$ is calculated by assuming nuclear vibrational modes are in thermal equilibrium with the surrounding at a temperature T (see Appendix B for the details). In the calculations, the energy is exchanged among the excitations while the total number of the electrons is conserved. The time-scale parameter $\delta\tau$ can be determined from the molecular mechanics simulation, and in this work is taken as a phenomenological parameter that is used to fit the experiments.

The geometry optimization, the nuclear vibrational modes, and their frequencies are obtained in the similar way as ref. 6 by a BLYP[7] calculation with 6-311G(d, p) basis set.[8] We find that the BLYP calculation yields much better optimized geometry and

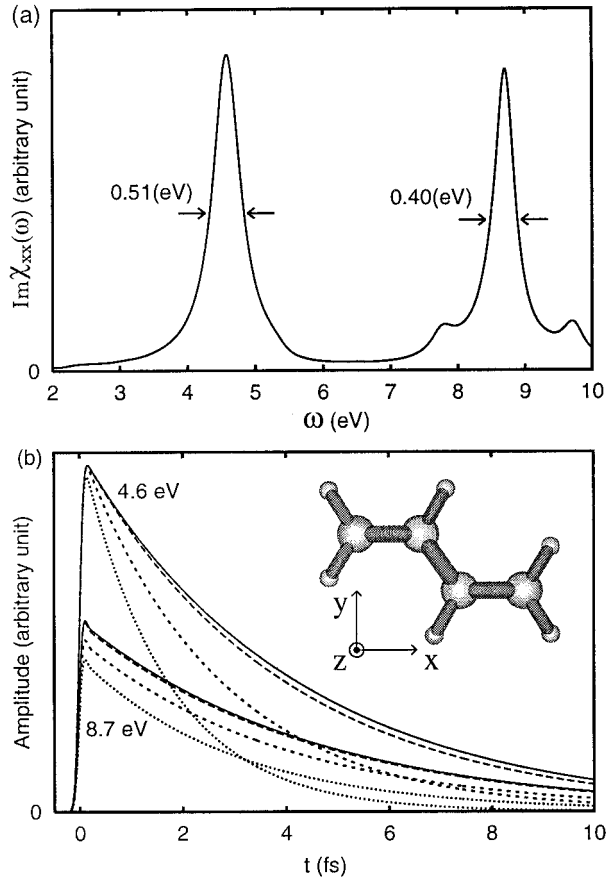

Figure 1. (a) Absorption spectrum at $T = 300$ K. (b) shows the relaxations of the two excitations (4.6 and 8.7 eV): amplitude of the mode vs. t. 1,3-Butadiene is placed as shown in the inset. Solid, long dashed, short dashed, and dotted line are for the 4.6 or 8.7 eV excitations at $T = 30$ K, $T = 100$ K, $T = 300$ K, and $T = 600$ K, respectively.

vibrational frequencies than the PM3 method. Therefore, in this work we adopt the optimized geometry, vibrational modes, and vibrational frequencies calculated by the BLYP method[7] with 6-311G(d, p) basis set.[8] In other words, $\hat{H}_B$ is determined by the BLYP calculation adopting 6-311G(d, p) basis set. The dipole matrix element $\vec{\mu}_{ij}$ is evaluated with the neglect of diatomic differential overlap (NDDO). The resulting 1,3-butadiene is placed in x-y plane as depicted in Figure 1. The electric pulse is expressed as $E(t) = E_0 \exp(-t/\bar{t})^2$ with $\bar{t} = 0.1$ fs, and its polarization is along the x-direction. Equation (12) is solved in the time domain. Temperature T is taken as 30, 100, 300, and 600 K, and $\delta\tau = 0.125$ fs is used. The absorption spectrum can be obtained by Fourier transforming the induced polarization $\vec{P}(t) = \mathrm{tr}[\vec{\mu}\delta\sigma(t)]$, and is plotted in Figure 1a for $T = 300$ K. The first peak appears at 4.6 eV, and its full-width-half-maximum (FWHM) is found to be 0.51 eV. The new formalism presented in this work includes the interactions between the valence electrons and all vibrational modes. This means that the calculated ΔE_{FWHM} correspond to homogeneous broadenings. The 0.51 eV FWHM of the first peak agrees approximately with the experimental measure of ~0.5 eV.[9] This is the reason why the value 0.125 fs of $\delta\tau$ is adopted in the calculations. Another major absorption peak is found at 8.7 eV, with a less FWHM of 0.40 eV. The different peak widths indicate the different decay rates of the two excitations at 4.6 and 8.7 eV. Figure 1b shows the amplitudes of the two excitation modes vs. time. The amplitudes are calculated by projecting the density matrix onto each modes of $\mathcal{M}^\mu$ [i.e., the eigenvector of eq. (12) in the absence of external field] as

$$\mathcal{P}^\mu(t) = \left| \sum_{i,j} ((\mathcal{M}^\mu)^{-1})_{ij} \delta\sigma_{ij}(t) \right|, \tag{21}$$

with

$$\sum_{i,j} |\mathcal{M}^\mu_{ij}|^2 = 1. \tag{22}$$

The decay half-time $\Delta\tau_{1/2}$ for 4.6 eV and 8.7 eV at temperature $T = 300$ K are 1.8 and 2.6 fs, respectively. It is verified that $\Delta E_{\mathrm{FWHM}} \Delta\tau_{1/2} \sim \hbar$ for the two excitations. Note that the 4.6 eV excitation decays always faster than the 8.7 eV excitation, especially at the high temperatures. The decay half-time of individual electronic excitation is found dependent on temperature T. This is because that the nuclear motion varies with changing temperature. In general, the increasing temperature leads the faster decays. The 4.6 eV excitation is more sensitive on T, and its decay rate increases much faster than the 8.7 eV excitation as T is raised. This is because that the 4.6 eV excitation couples more strongly to the nuclear motion, which is examined more closely below.

We can evaluate the couplings between the electronic excitations and nuclear vibrational modes by recasting eq. (12) as follows,

$$i\hbar \frac{d}{dt} \delta\sigma_{ij} = \sum_{k,l} \mathcal{L}_{ijkl} \delta\sigma_{kl} + [f, \sigma^{(0)}]_{ij} - i\delta\tau \sum_{k,l,\nu} \coth\left(\frac{\beta\hbar\omega_\nu}{2}\right) \bar{\Gamma}^\nu_{ijkl} \delta\sigma_{kl}, \tag{23}$$

where $\mathcal{L}_{ijkl}$ is defined in eq. (A2) and

$$\bar{\Gamma}^\nu_{ijkl} = \frac{1}{\hbar} \left(\sum_m \bar{K}^\nu_{im} \bar{K}^\nu_{mk} \delta_{jl} + \sum_m \delta_{ik} \bar{K}^\nu_{lm} \bar{K}^\nu_{mj} - 2\bar{K}^\nu_{ik} \bar{K}^\nu_{lj} \right), \tag{24}$$

where $\bar{K}^\nu$ is similar to K^ν but does not have its temperature dependence,

$$\bar{K}^\nu_{ij} \equiv \sum_{m,s} \frac{\partial t_{ij}}{\partial q_{ms}} \sqrt{\frac{\hbar}{2M_m\omega_\nu}}\, Q^\nu_{ms}. \tag{25}$$

To examine the couplings between the electronic excitations and nuclear vibrations, we rewrite eq. (23) in the harmonic oscillator

(HO) representation.[10,11] Transformation matrix $S_{ij,\alpha}$ between the site and HO representations is given by

$$S_{ij,\alpha} = \begin{cases} (\mathcal{M}_0^{\alpha})_{ij} & \alpha\varepsilon \text{ electron-hole or hole-electron,} \\ \mathcal{V}_{\alpha,ij} & \alpha\varepsilon \text{ electron-electron or hole-hole,} \end{cases} \quad (26)$$

where electron and hole stand for the unoccupied HF levels and occupied HF levels, respectively, and $\mathcal{V}_{\alpha,ij}$ is given by the HF molecular orbital coefficient c_{im} defined in eq. (A12):

$$\mathcal{V}_{\alpha,ij} = c_{im}c_{jn}, \quad \alpha = (mn). \quad (27)$$

By using $S_{ij,\alpha}$, eq. (23) is rewritten as

$$i\hbar \frac{d}{dt} \sum_{i,j} (S^{-1})_{\alpha,ij}\delta\sigma_{ij} = \sum_{i,j,k,l,m,n,\alpha'} (S^{-1})_{\alpha,ij}\mathcal{L}_{ijkl}S_{kl,\alpha'}(S^{-1})_{\alpha',mn}\delta\sigma_{mn} + \sum_{i,j} (S^{-1})_{\alpha,ij}[f, \sigma^{(0)}]_{ij} - i\delta\tau \sum_{i,j,k,l,m,n,\nu,\alpha'} \coth\left(\frac{\beta\hbar\omega_\nu}{2}\right) \times (S^{-1})_{\alpha,ij}\bar{\Gamma}^{\nu}_{ijkl}S_{kl,\alpha'}(S^{-1})_{\alpha',mn}\delta\sigma_{mn}. \quad (28)$$

Thus, we obtain the following equation.

$$i\hbar \frac{d}{dt} \delta\sigma_\alpha = \sum_{\alpha'} \mathcal{L}_{\alpha\alpha'}\delta\sigma_{\alpha'} + \sum_{i,j} (S^{-1})_{\alpha,ij}[f, \sigma^{(0)}]_{ij} - i\delta\tau \sum_{\nu,\alpha'} \coth\left(\frac{\beta\hbar\omega_\nu}{2}\right)\bar{\Gamma}^{\nu}_{\alpha\alpha'}\delta\sigma_{\alpha'}, \quad (29)$$

where σ_α, $\mathcal{L}_{\alpha\alpha'}$, and $\bar{\Gamma}^{\nu}_{\alpha\alpha'}$ are given by

$$\delta\sigma_\alpha = \sum_{i,j} (S^{-1})_{\alpha,ij}\delta\sigma_{ij}, \quad (30)$$

$$\mathcal{L}_{\alpha\alpha'} = \sum_{i,j,k,l} (S^{-1})_{\alpha,ij}\mathcal{L}_{ijkl}S_{kl,\alpha'}, \quad (31)$$

$$\bar{\Gamma}^{\nu}_{\alpha\alpha'} = \sum_{i,j,k,l} (S^{-1})_{\alpha,ij}\bar{\Gamma}^{\nu}_{ijkl}S_{kl,\alpha'}. \quad (32)$$

The third term on the RHS of eq. (29) describes the coupling between the electronic mode α and α' through the vibrational mode ν. The magnitude of $\delta\tau \sum_\nu \coth(\beta\hbar\omega_\nu/2)\bar{\Gamma}^{\nu}_{\alpha\alpha'}$ in eq. (29) determines the decay rate for the α-th electronic mode. A set of $\bar{\Gamma}^{\nu}_{\alpha\alpha'}$ for the several electron-hole modes are shown in Table 1. Vibrational modes are arranged from top to bottom with increasing order of energy. Electronic modes $\mathcal{M}_0^{122}$ and $\mathcal{M}_0^{144}$ correspond to the peaks at 4.6 and 8.7 eV in Figure 1, respectively. The diagonal terms $\bar{\Gamma}_{\alpha,\alpha}$ are the pure dephasing for mode α, and are much larger than the off-diagonal terms. The large pure dephasing is likely due to all the couplings between the electronic excitation and different phonons that destroy the electronic phase coherence. $\bar{\Gamma}^{\nu}_{122,122}$ is large for lower vibrational frequency modes and generally very small for higher vibrational modes, while in contrast, $\bar{\Gamma}^{\nu}_{144,144}$ shows a less vibrational frequency dependence. This leads to the different decay behaviors for the two excitations, as shown in Figure 1b. For very lower temperature ($\beta \to \infty$), $\coth(\beta\hbar\omega_\nu/2) \sim 1$ irrespective of ν. Because the ratio $\Sigma_\nu \bar{\Gamma}^{\nu}_{122,122}/\Sigma_\nu \bar{\Gamma}^{\nu}_{144,144}$ is about 1.2, the decay rates of the 4.6 and 8.7 eV excitations are thus similar. For high temperatures, i.e., $\beta\hbar\omega_\nu \ll 1$, $\coth(\beta\hbar\omega_\nu/2) \sim 1/\beta\hbar\omega_\nu = k_BT/\hbar\omega_\nu$. Thus, the low-frequency vibrational modes dominate the contribution to the dissipation. Further $\bar{\Gamma}^{\nu_{13}}_{122,122}/\bar{\Gamma}^{\nu_{13}}_{144,144} \sim 2.8$, the 4.6 eV excitation decays thus much faster than the 8.7 eV one at high temperatures.

Table 1. Coupling Strength between Electronic Excitations and Nuclear Vibrational Modes.

	ν	ω_ν (cm^{-1})	$\bar{\Gamma}^{\nu}_{122,122}$	$\bar{\Gamma}^{\nu}_{122,144}$	$\bar{\Gamma}^{\nu}_{144,144}$
1	ν_{13} Au	173.1	0.429	−0.050	0.153
2	ν_{24} Bu	294.3	0.003	0.012	0.067
3	ν_{9} Ag	508.0	0.003	0.007	0.034
4	ν_{12} Au	520.9	0.228	0.019	0.114
5	ν_{16} Bg	755.7	0.173	0.020	0.071
6	ν_{8} Ag	876.9	0.009	0.005	0.059
7	ν_{11} Au	888.8	0.179	−0.008	0.039
8	ν_{15} Bg	892.4	0.177	−0.006	0.041
9	ν_{14} Bg	963.3	0.111	−0.001	0.050
10	ν_{23} Bu	981.6	0.003	0.011	0.058
11	ν_{10} Au	1025.1	0.096	0.005	0.039
12	ν_{7} Ag	1194.3	0.018	0.008	0.046
13	ν_{6} Ag	1280.8	0.014	0.005	0.036
14	ν_{22} Bu	1288.6	0.006	0.009	0.040
15	ν_{21} Bu	1379.3	0.009	0.001	0.037
16	ν_{5} Ag	1439.7	0.008	0.008	0.049
17	ν_{20} Bu	1593.6	0.040	−0.012	0.053
18	ν_{4} Ag	1633.5	0.098	0.006	0.059
19	ν_{3} Ag	3037.6	0.003	0.010	0.034
20	ν_{19} Bu	3048.9	0.003	0.010	0.030
21	ν_{2} Bu	3053.9	0.002	0.005	0.043
22	ν_{18} Ag	3055.0	0.002	0.006	0.043
23	ν_{1} Ag	3137.0	0.002	0.011	0.070
24	ν_{17} Bu	3137.3	0.002	0.011	0.070

Vibrational modes are arranged from top to bottom with increasing order of energy. $\bar{\Gamma}^{\nu}_{\alpha\alpha'}$ is given in eV/fs. Electronic excitation modes $\mathcal{M}_0^{122}$ and $\mathcal{M}_0^{144}$ correspond to the peaks at 4.6 and 8.7 eV in Figure 1, respectively.

Figure 2 shows the population relaxation after the incidence of a weak electric pulse by solving eq. (10). The density matrix $\delta\sigma$ is mapped onto the Hartree–Fock molecular orbital representation,[10] and the induced populations of the highest occupied molecular orbital (HOMO), HOMO − 1, HOMO − 2, the lowest unoccupied molecular orbital (LUMO), LUMO + 1, and LUMO + 2 are plotted vs. time t. The negative value indicates the depletion of the electron or the existence of holes. The induced populations of the HOMO and LUMO (also HOMO − 1 and LUMO + 1) are almost the mirror images of each other, while the populations of the HOMO − 2 and LUMO + 2 are completely different. The larger numbers of induced electrons (holes) at the LUMO (HOMO) indicates the efficient transition of electrons from the HOMO to the LUMO immediately after the application of the electric pulse $E(t)$. All the induced populations (electrons or holes) decay to zero, i.e., the molecule relaxes to the ground state. The population

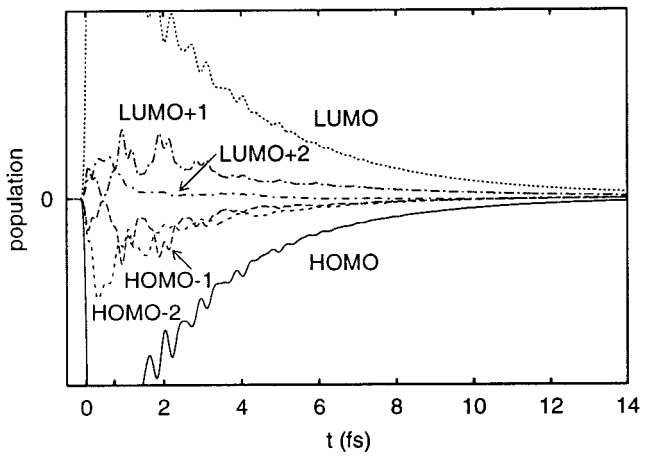

Figure 2. The population relaxations for HOMO, LUMO, HOMO − 1, LUMO + 1, HOMO − 2, and LUMO + 2. The solid line (HOMO), for example, shows $\delta\sigma_{\mathrm{HOMO,HOMO}}$ vs. time t in Hartree–Fock molecular orbital representation.[10]

relaxation to the ground state is due to the existence of the electron–hole (hole–electron) coupling components of matrix K^{ν}.

Discussion

We have shown that the new formalism can be employed to simulate the nonradiative relaxations of realistic many-electron molecular systems that are in contact with thermal baths. Various excitations may couple differently to the thermal bath, and this is taken into account naturally by the new formalism. The Markovian TDHF-QDT developed here is essentially the same as the formula presented in ref. 12, although the derivations are seemingly different. Inclusion of radiative decay process into the equation of motion should be straightforward. The different time scales are required for radiative and nonradiative decays. Explicit inclusion of the nuclear vibrational modes and/or multiconfigurational effect to the current scheme is challenging but feasible.

We set out to achieve two objectives. The first objective is to demonstrate the applicability of TDHF-QDT to real molecular systems. Our simulation has clearly captured the essential physics of the nonradiative decay of a butadiene molecule, for instance, the rate dependence on temperature and different decay rates for different excited states that were not built into the theory phenomenologically but are rather the nature consequences of the dissipation terms derived directly from the Hamiltonian. The first objective is thus achieved with success. The second objective is to examine the decaying processes of the embedded butadiene molecule upon photoexcitation. This is carried out under the Markovian approximation. Our simulation predicts that the excitation at 4.6 eV decays rapidly at room temperature and its decay rate is sensitive to the temperature because it couples strongly with the low-frequency vibrational modes. The validity of this prediction rests on the Markovian approximation, and should be tested experimentally. The Markovian version of the TDHF-QDT was used in the simulation instead of the non-Markovian TDHF-QDT, because the former is computationally less expensive. We assume the system-bath factorization ansatz and use the Hartree–Fock ground state for the system ground state. The energy dissipation causes the energy exchange between the electrons and nuclei, and leads to the deterioration of the Hartree–Fock approximation. An improved approach is to find the equilibrium state under the system-bath couplings and thermal fluctuations as we did in ref. 1. Our equation does not consider the large amplitude motion and photoisomerization. Those effects are beyond the scope of this work, which is intended to develop and illustrate the applicability of the TDHF-QDT formalism for realistic open systems. The Franck–Condon calculation of the absorption spectrum requires the explicit determination of excited states and their energy surfaces. In the present implementation the vibronic structure cannot be evaluated because the vibrational modes are not included in the system. This can be achieved by including the nuclei as a part of the system.

It is emphasized that this formalism is based on the EOM of reduced single-electron density matrix, and is very different from the conventional QDTs that follow the dynamics of the reduced density matrix of system. Therefore, this formalism can be applied for much larger and realistic systems, as we did here. In our calculation, we include explicitly all valence electrons (total of 22 electrons) and take into account the couplings between all valence electrons and all vibrational modes. For most conventional QDTs, one solves the electronic structures first and then adds T_1 and T_2 relaxation terms phenomenologically.[13,14] In principle, the T_1 and T_2 relaxation terms can be evaluated explicitly.[14] However, because of extremely large computational resources are required, this has not been done for realistic many-electron systems.[14] Utilizing the locality of $\langle \hat{F}_a \hat{F}_b \rangle$, eq. (6) can be combined with the localized density-matrix (LDM) method.[15] This leads the dramatic reduction of computational times, and thus the possibility of simulating very large complex open molecular systems.

To conclude, we have demonstrated that our dynamic mean field QDT can be readily applied to simulate the realistic quantum dissipative molecular systems. Our formalism introduces for the first time the quantum chemistry methodology to simulate directly the dissipative many-electron systems. For the moment, it employs the semiempirical Hamiltonian. We can implement easily our formalism with the first-principle quantum chemistry methods, for instance, the time-dependent density functional theory (TD-DFT).[16] This would make the first-principle simulations of realistic open molecular systems possible.

Appendix A: Numerical Stability of Eq. (12)

Unlike the Lindblad equation where the equation of motion is linear equation of the reduced density matrix of the system, eq. (10) is a nonlinear equation of motion of $\sigma(t)$. Thus, it is not clear whether $\delta\sigma(t)$ does not grow with time according to eq. (10). We show here that $\delta\sigma(t)$ does not grow unphysically or eq. (12) is numerically stable as long as the excitations are weak.

Let us rewrite eq. (12) in the absence of the external field as follows,

$$i\hbar \frac{d}{dt} \delta\sigma_{ij} = \sum_{i,j} \mathcal{L}_{ijkl}\delta\sigma_{kl} - \frac{i}{\hbar} \delta\tau \sum_{i,j} \mathcal{A}_{ijkl}\delta\sigma_{kl} \tag{A1}$$

where linearized Liouville operator $\mathcal{L}$ and linearized dissipative operator $\mathcal{A}$ are given by

$$\mathcal{L}_{ijkl} = h^{(0)}_{ik}\delta_{j,l} - \delta_{i,k}h^{(0)}_{lj} + \sum_{m} \{(v_{im,lk} - v_{ik,lm})\sigma^{(0)}_{mj} - \sigma^{(0)}_{im}(v_{mj,lk} - v_{mk,lj})\}, \tag{A2}$$

$$\mathcal{A}_{ijkl} = \sum_{\nu} \left(\sum_{m} K^{\nu}_{im}K^{\nu}_{mk}\delta_{jl} + \sum_{m} \delta_{ik}K^{\nu}_{lm}K^{\nu}_{mj} - 2K^{\nu}_{ik}K^{\nu}_{lj} \right) \tag{A3}$$

and K^{ν} in eq. (20) is replaced by

$$K^{\nu}_{ij} \equiv \sum_{m,s} \frac{\partial t_{ij}}{\partial q_{ms}} \sqrt{\frac{\hbar}{2M_m\omega_{\nu}} \coth\left(\frac{\beta\hbar\omega_{\nu}}{2}\right)} Q^{\nu}_{ms}. \tag{A4}$$

Here, it does not depend on σ. Equation (A1) has the Lindblad-like form except the terms in the summation in eq. (A2). The solution of eq. (A1) can be formally obtained with the initial condition of $\delta\sigma$ as $\delta\sigma_I$:

$$\delta\sigma(t) = \exp\left(-\frac{i}{\hbar}\mathcal{L}t - \frac{\delta\tau}{\hbar^2}\mathcal{A}t \right)\delta\sigma_I. \tag{A5}$$

To ensure $\delta\sigma \to 0$ as $t \to \infty$, all the eigenvalue Ω_{α} of the super operator $-i/\hbar\mathcal{L} - \delta\tau/\hbar^2\mathcal{A}$ have to satisfy $\mathrm{Re}(\Omega_{\alpha}) \leq 0$.

Our proof is made by the following steps: (a) showing the positivity of the dissipation superoperator $\mathcal{A}$, i.e., all the eigenvalues of $\mathcal{A}$ are positive, (b) showing that the eigenvalue of adiabatic TDHF equation is real, and (c) showing $\delta\sigma(t)$ does not grow with time.

(a) We show that all the eigenvalues of $\mathcal{A}$ are positive as follows. Because K^{ν} is a real symmetric matrix in the calculation, $\mathcal{A}_{ijkl}$ is real symmetric in terms of the exchange of a set of the indices $(i, j) \leftrightarrow (k, l)$. As a result, $\mathcal{A}$ can be diagonalized by a real orthogonal matrix in Liouville space. In more general cases, K^{ν} can be a Hermitian matrix. Correspondingly, $\mathcal{A}$ will be Hermitian matrix in terms of the exchange of a set of the indices $(i, j) \leftrightarrow (k, l)$. We denote the eigenvalue and eigenvector as Γ_{ν} and $e_{\nu,ij}$. Any matrix J_{ij} can be expanded by the eigenvector $e_{\nu,ij}$

$$J_{ij} = \sum_{\nu} a_{\nu}e_{\nu,ij}, \quad J^*_{ij} = \sum_{\nu} a^*_{\nu}e^*_{\nu,ij} \tag{A6}$$

where the asterisk is for the complex conjugate. Now we define the following function.

$$D(J) \equiv \sum_{i,j,k,l} J^*_{ij}\mathcal{A}_{ijkl}J_{kl}. \tag{A7}$$

From eq. (A6) we have

$$D(J) = \sum_{i,j,k,l} \sum_{\nu} a^*_{\nu}e^*_{\nu,ij}\mathcal{A}_{ijkl} \sum_{\xi} a_{\xi}e_{\xi,kl} = \sum_{i,j} \sum_{\nu,\xi} a^*_{\nu}a_{\xi}e^*_{\nu,ij}\Gamma_{\xi}e_{\xi,ij} = \sum_{\nu,\xi} a^*_{\nu}a_{\xi}\delta_{\nu,\xi}\Gamma_{\xi} = \sum_{\nu} |a_{\nu}|^2\Gamma_{\nu}. \tag{A8}$$

If $D(\delta\sigma) \geq 0$ for any $\delta\sigma$, $\Gamma_{\nu} \geq 0$ have to be satisfied for all ν. By inserting the explicit form of $\mathcal{A}$ in eq. (A3) to eq. (A7), we have

$$D(J) = \sum_{\nu} \mathrm{Tr}(J^{\dagger}K^{\nu}K^{\nu}J + J^{\dagger}JK^{\nu}K^{\nu} - 2J^{\dagger}K^{\nu}JK^{\nu}). \tag{A9}$$

Denote

$$\Xi^{\nu}_1 = JK^{\nu}, \quad \Xi^{\nu}_2 = J^{\dagger}K^{\nu}. \tag{A10}$$

Then eq. (A9) is written as

$$D(J) = \sum_{\nu} \mathrm{tr}(\Xi^{\nu}_2\Xi^{\nu\dagger}_2 + \Xi^{\nu}_1\Xi^{\nu\dagger}_1 - \Xi^{\nu}_2\Xi^{nu}_1 - \Xi^{\nu\dagger}_2\Xi^{\nu\dagger}_1) = \sum_{\nu} \mathrm{tr}[(\Xi^{\nu}_2 - \Xi^{\nu\dagger}_1)(\Xi^{\nu\dagger}_2 - \Xi^{\nu}_1)] = \sum_{\nu} \mathrm{tr}|\Xi^{\nu}_2 - \Xi^{\nu\dagger}_1|^2 \geq 0. \tag{A11}$$

Therefore, all the eigenvalue satisfy $\Gamma_{\nu} \geq 0$. Equality holds for σ which commutes with K_{ν} for all ν. Unit matrix I is one of such example.

(b) $\mathcal{L}$ can be diagonalized[10,11,17] as follows. First, we find the HF energy ε_k and molecular orbital coefficient c_{mk} from the HF equation.

$$\sum_{n} h^{(0)}_{mn}\phi_{nk} = \varepsilon_k\phi_{mk}. \tag{A12}$$

Then, we define the transformation matrix $\mathcal{V}$ from site representation to HFMO representation

$$\mathcal{V}_{k,l,m,n} = \phi_{mk}\phi_{nl} \tag{A13}$$

which satisfies the condition

$$\mathcal{V}^{-1} = \mathcal{V}^{\dagger}. \tag{A14}$$

The linearized Liouville operator in HFMO representation $\mathcal{L}$ is calculated by

$$\tilde{\mathcal{L}} = \mathcal{V}\mathcal{L}\mathcal{V}^{\dagger}. \tag{A15}$$

$\tilde{\mathcal{L}}$ has the following form:

$$\tilde{\mathcal{L}} = \begin{pmatrix} \tilde{\mathcal{L}}_{11} & \tilde{\mathcal{L}}_{12} \\ 0 & \tilde{\mathcal{L}}_{22} \end{pmatrix} \tag{A16}$$

where $\tilde{\mathcal{L}}_{11}$, $\tilde{\mathcal{L}}_{22}$, and $\tilde{\mathcal{L}}_{12}$ are corresponding to the matrix elements among (electron–hole, hole–electron) part, among (hole–hole, electron–electron) part, and between (electron–hole, hole–electron) and (hole–hole, electron–electron) part, respectively. $\tilde{\mathcal{L}}_{22}$ is

a diagonal matrix: $(\tilde{\mathscr{L}}_{22})_{e,e',e'',e'''} = \delta_{e,e''}\delta_{e',e'''}(\Omega_2)_{e,e'}$ and $(\tilde{\mathscr{L}}_{22})_{h,h',h'',h'''} = \delta_{h,h''}\delta_{h',h'''}(\Omega_2)_{h,h'}$ with

$$(\Omega_2)_{e,e'} = \varepsilon_e - \varepsilon_{e'}, \quad (\Omega_2)_{h,h'} = \varepsilon_h - \varepsilon_{h'} \tag{A17}$$

where e (e') and h (h') correspond to electron and hole indices, respectively. $\tilde{\mathscr{L}}_{11}$ and $\tilde{\mathscr{L}}_{12}$ are written with the Coulomb interactions in MO representation $\tilde{v}$

$$\tilde{v}_{p_1,p_2,p_3,p_4} = \sum_{i,j,k,l} (\mathscr{V})_{p_1,p_2,i,j}(\mathscr{V}^\dagger)_{k,l,p_3,p_4} \times \sum_m \{(v_{im,lk} - v_{ik,lm})\sigma^{(0)}_{mj} - \sigma^{(0)}_{im}(v_{mj,lk} - v_{mk,lj})\}, \tag{A18}$$

$$(\tilde{\mathscr{L}}_{11})_{eh,e'h'} = (\varepsilon_e - \varepsilon_h)\delta_{ee'}\delta_{hh'} + \tilde{v}_{eh,e'h'}, \tag{A19a}$$

$$(\tilde{\mathscr{L}}_{11})_{h,e,e',h'} = \tilde{v}_{h,e,e',h'}, \tag{A19b}$$

$$(\tilde{\mathscr{L}}_{11})_{e,h,h',e'} = -(\mathscr{L}_{11})_{h,e,e',h'}, \tag{A19c}$$

$$(\tilde{\mathscr{L}}_{11})_{h,e,h',e'} = -(\mathscr{L}_{11})_{e,h,e',h'}, \tag{A19d}$$

$$(\tilde{\mathscr{L}}_{12})_{e,h,h',h''} = \tilde{v}_{e,h,h',h''}, \tag{A19e}$$

$$(\tilde{\mathscr{L}}_{12})_{h,e,h',h''} = -(\tilde{\mathscr{L}}_{12})_{e,h,h',h''}, \tag{A19f}$$

$$(\tilde{\mathscr{L}}_{12})_{e,h,e',e''} = \tilde{v}_{e,h,e',e''}, \tag{A19g}$$

$$(\tilde{\mathscr{L}}_{12})_{h,e,e',e''} = -(\tilde{\mathscr{L}}_{12})_{e,h,e',e''}. \tag{A19h}$$

$\tilde{\mathscr{L}}_{11}$ can be diagonalized by a matrix w

$$w\tilde{\mathscr{L}}_{11}w^{-1} = \Omega_1, \tag{A20}$$

where the matrix w has a form

$$w = \begin{pmatrix} X & -Y \\ Y & -X \end{pmatrix}, \quad w^{-1} = \begin{pmatrix} X^\dagger & -Y^\dagger \\ Y^\dagger & -X^\dagger \end{pmatrix}, \tag{A21}$$

with

$$w_{\sigma,e,h} = X_{\sigma,e,h} \tag{A22}$$

$$w_{\sigma,h,e} = -Y_{\sigma,e,h} \tag{A23}$$

$$w_{\bar{\sigma},e,h} = Y_{\sigma,e,h} \tag{A24}$$

$$w_{\bar{\sigma},h,e} = -X_{\sigma,e,h} \tag{A25}$$

and $(\Omega_1)_\sigma > 0$, $(\Omega_1)_{\bar{\sigma}} = -(\Omega_1)_\sigma$.

Unlike the TDHF method where electron–electron and hole–hole part are determined by electron–hole and hole–electron part, electron–electron and hole–hole part in eq. (A1) are independent valuables and couple with electron–hole and hole–electron part from the linear order of the optical response. Thus, we have to consider the effect of $\tilde{\mathscr{L}}_{12}$. This can easily be done by the following matrix w':

$$w' = \begin{pmatrix} I & \mathscr{M} \\ 0 & I \end{pmatrix}, \quad w'^{-1} = \begin{pmatrix} I & -\mathscr{M} \\ 0 & I \end{pmatrix}, \tag{A26}$$

where I is the unit matrix and $\mathscr{M}$ is given by

$$(\mathscr{M})_{\sigma,e,e'} = \frac{(w\tilde{\mathscr{L}}_{12})_{\sigma,e,e'}}{(\Omega_1)_\sigma - (\Omega_2)_{e,e'}}, \tag{A27}$$

$$(\mathscr{M})_{\sigma,e,e'} = \frac{(w\tilde{\mathscr{L}}_{12})_{\bar{\sigma},e,e'}}{-(\Omega_1)_\sigma - (\Omega_2)_{e,e'}}, \tag{A28}$$

$$(\mathscr{M})_{\sigma,h,h'} = \frac{(w\tilde{\mathscr{L}}_{12})_{\sigma,h,h'}}{(\Omega_1)_\sigma - (\Omega_2)_{h,h'}}, \tag{A29}$$

$$(\mathscr{M})_{\sigma,h,h'} = \frac{(w\tilde{\mathscr{L}}_{12})_{\bar{\sigma},h,h'}}{-(\Omega_1)_\sigma - (\Omega_2)_{h,h'}}. \tag{A30}$$

Finally, after defining the following matrix w_0 in Liouville space

$$w_0 = \begin{pmatrix} w & 0 \\ 0 & I \end{pmatrix}, \quad w_0^{-1} = \begin{pmatrix} w^{-1} & 0 \\ 0 & I \end{pmatrix} \tag{A31}$$

we have the following eigenvalues for $\mathscr{L}$

$$(w'w_0\mathscr{V}\mathscr{L}\mathscr{V}^t w_0^{-1}w'^{-1})_{\nu,\nu'} = \delta_{\nu,\nu'}\Omega_\nu \tag{A32}$$

with $\Omega_\sigma = (\Omega_1)_\sigma$, $\Omega_{\bar{\sigma}} = (\Omega_1)_{\bar{\sigma}}$, $\Omega_{e,e'} = (\Omega_2)_{e,e'}$, and $\Omega_{h,h'} = (\Omega_2)_{h,h'}$. Therefore, all the eigenvalues of $\mathscr{L}$ are real.

(c) Now we are ready to prove that $\delta\sigma_{ij}$ in eq. (A1) is a decay function of time. We use Trotter formula[18] on eq. (A5).

$$\begin{aligned}\delta\sigma(t) &= \lim_{n\to\infty}\left(\exp\left(-\frac{i}{\hbar}\mathscr{L}\frac{t}{n}\right)\exp\left(-\frac{\delta\tau}{\hbar^2}\mathscr{A}\frac{t}{n}\right)\right)^n \delta\sigma_I \\ &= \lim_{n\to\infty}\sum_{\mu_1\nu_1}\cdots\sum_{\mu_n\nu_n}\prod_{i=1}^{n}(\beta^{i\nu_i}_{\mu_i}\alpha^{i\nu_{i-1}}_{\mu_i})\eta^n_{\nu_n} \times \exp\left(-\frac{i}{\hbar}(\Omega_{\nu_1} + \cdots + \Omega_{\nu_n})\frac{t}{n}\right) \times \exp\left(-\frac{\delta\tau}{\hbar^2}(\Gamma_{\mu_1} + \cdots + \Gamma_{\mu_n})\frac{t}{n}\right),\end{aligned} \tag{A33}$$

where $\alpha^{i\nu_{i-1}}_{\mu_i}$ and $\beta^{i\nu_i}_{\mu_i}$ are expansion coefficients defined as

$$\eta_{\nu_{i-1}} = \sum_{\mu_i}\alpha^{i\nu_{i-1}}_{\mu_i}\xi_{\mu_i}, \tag{A34}$$

$$\xi_{\mu_i} = \sum_{\nu_i}\beta^{i\nu_i}_{\mu_i}\eta_{\nu_i} \tag{A35}$$

where $\eta_{\nu_0} = \delta\sigma_I$ and ξ_{μ_i} and η_{ν_i} are eigenvector of $\mathscr{A}$ and right eigenvector of $\mathscr{L}$. $\beta^{i\nu_i}_{\mu_i}$ can be calculated by the left eigenvector $\tilde{\eta}$ of $\mathscr{L}$.

$$\beta_{\mu_i}^{i\nu_i} = \sum_{m,n} (\tilde{\eta}_{\nu_i})_{m,n} (\xi_{\mu_i})_{m,n}. \tag{A36}$$

Because of the number conservation $i\hbar d/dt \sum_j \sigma_{jj} = 0$, $\delta\sigma$ should not have any unit matrix component. We first assume that any $\delta\sigma$ does not commute with K^ν. Therefore, $\Gamma_{\mu_i} > 0$ for nonzero $\alpha_{mu_i}^{\nu_{i-1}}$. We set the smallest nonzero Γ_{μ_i} as γ_0. Then we get the following inequality.

$$\delta\sigma(t) \le \lim_{n\to\infty} \sum_{\mu_1\nu_1} \cdots \sum_{\mu_n\nu_n} \prod_{i=1}^{n} (\beta_{\mu_i}^{i\nu_i} \alpha_{\mu_i}^{i\nu_{i-1}}) \eta_{\nu_n}^n \times \exp\left(-\frac{i}{\hbar} (\Omega_{\nu_1} + \cdots + \Omega_{\nu_n}) \frac{t}{n} \right) \times \exp\left(-\frac{\delta\tau}{\hbar^2} \gamma_0 t \right). \tag{A37}$$

On the other hand, the time evolution of the TDHF in the linear order of optical response can be written as

$$\delta\tilde{\sigma}(t) = \exp\left(-\frac{i}{\hbar} \mathcal{L} t \right) \delta\sigma_I = \lim_{n\to\infty} \sum_{\mu_1\nu_1} \cdots \sum_{\mu_n\nu_n} \prod_{i=1}^{n} (\beta_{\mu_i}^{i\nu_i} \alpha_{\mu_i}^{i\nu_{i-1}}) \eta_{\nu_n}^n \times \exp\left(-\frac{i}{\hbar} (\Omega_{\nu_1} + \cdots + \Omega_{\nu_n}) \frac{t}{n} \right). \tag{A38}$$

Thus, we have

$$\delta\sigma(t) \le \delta\tilde{\sigma}(t) \exp\left(-\frac{\delta\tau}{\hbar^2} \gamma_0 t \right). \tag{A39}$$

Because the amplitude of the oscillation of $\delta\tilde{\sigma}(t)$ does not change with time, $\delta\sigma(t)$ decay to zero for $t \to \infty$. Next we assume that one of the ξ_μ commutes with all K_ν. Even in this case, if ξ_μ is not the eigenvector of $\mathcal{L}\delta\sigma$ still decays with time, because $\exp(-i\mathcal{L}t/(\hbar n))$ mix ξ_μ with other eigenvectors and other eigenvector decays as shown in eq. (A39). Only in the case where ξ_μ commutes with all K_ν and it is the eigenvector of both $\mathcal{A}$ and $\mathcal{L}$, ξ_μ component of $\delta\sigma$ does not decay with time.

Appendix B: Derivation of Nuclear Correlation Function

In Equation (17) we make the following transformation,

$$x_i = \sum_{j,s} Q_{i,(js)} \sqrt{\frac{M_j}{2}}\, \delta\tilde{q}_{js} \tag{B1}$$

where $Q_{i,(js)}$ is the orthonormal matrix that satisfies the following relation.

$$\sum_{i_1,i_2,s_1s_2} Q_{j,(i_1s_1)} \frac{V_{i_1s_1,i_2s_2}}{\sqrt{M_{i_1}M_{i_2}}} (Q^\dagger)_{(i_2s_2),k} = \delta_{j,k} \bar{V}_k. \tag{B2}$$

With using the new variable x_i, the bath Hamiltonian H_n in eq. (17) is written as

$$H_n = \sum_i \left(-\frac{\hbar^2}{4} \frac{\partial^2}{\partial x_i^2} + \bar{V}_i x_i^2 \right). \tag{B3}$$

Because each x_i is harmonic oscillator, we can solve the Schrödinger equation by the separation of variables.

$$\left(-\frac{\hbar^2}{4} \frac{\partial^2}{\partial x_i^2} + \bar{V}_i x_i^2 \right) \psi_{n_i}(x_i) = \mathcal{E}_{n_i} \psi_{n_i}(x_i). \tag{B4}$$

where energy eigenvalue is given as $\mathcal{E}_{n_i} = \hbar\omega_i(n + 1/2)$ with $\omega_i = \sqrt{\bar{V}_i}$. Its mean square amplitude is obtained as

$$\int dx_i \psi_{n_i}^\dagger(x_i)\, x_i^2 \psi_{n_i}(x_i) = \frac{\hbar}{2\omega_i} \left(n_i + \frac{1}{2} \right). \tag{B5}$$

We denote the total energy and wavefunction by $\mathcal{E}_\lambda^T$ and Ψ_λ with the index λ is for combination of all the modes, i.e., $\lambda = (n_1, n_2, n_3, \ldots, n_{3N-6})$. Wave function is thus given by $\Psi_\lambda = \prod_i \psi_{n_i}(x_i)$. Statistical average is then done as follows:

$$\langle x_i x_j \rangle = \frac{\sum_\lambda \int \prod_k dx_k \Psi_\lambda^\dagger x_i x_j e^{-\beta\mathcal{E}_\lambda^T} \Psi_\lambda}{\sum_\lambda \int \prod_k dx_k \Psi_\lambda^\dagger e^{-\beta\mathcal{E}_\lambda^T} \Psi_\lambda} = \delta_{i,j} \frac{\sum_{n_i} \int dx_i \psi_{n_i}^\dagger x_i^2 e^{-\beta\mathcal{E}_{n_i}} \psi_{n_i}}{\sum_{n_i} \int dx_i \psi_{n_i}^\dagger e^{-\beta\mathcal{E}_{n_i}} \psi_{n_i}}$$

$$= \delta_{i,j} \frac{\sum_{n_i=0}^{\infty} \frac{\hbar}{2\omega_i} \left(n_i + \frac{1}{2} \right) e^{-\beta\hbar\omega_i n_i}}{\sum_{n_i=0}^{\infty} e^{-\beta\hbar\omega_i n_i}} = \delta_{i,j} \frac{\hbar}{4\omega_i} \coth\left(\frac{\beta\hbar\omega_i}{2} \right). \tag{B6}$$

From eq. (B1) and (B6) we obtain

$$\langle \delta\tilde{q}_{i_1s_1} \delta\tilde{q}_{i_2s_2} \rangle = \frac{1}{\sqrt{M_{i_1}M_{i_2}}} \sum_k (Q^\dagger)_{(i_1s_1),k} (Q^\dagger)_{(i_2s_2),k} \times \frac{\hbar}{2\omega_k} \coth\left(\frac{\beta\hbar\omega_k}{2} \right). \tag{B7}$$

References

1. Yokojima, S.; Chen, G. H.; Xu, R.; Yan, Y. J. Chem Phys Lett 2003, 369, 495.
2. Xu, R.; Yan, Y. J Chem Phys 2002, 116, 9196.
3. Meier, C.; Tannor, D. J. J Chem Phys 1999, 111, 3365.
4. Lindblad, G. Commun Math Phys 1976, 48, 119; Lindblad, G. Rep Math Phys 1976, 10, 393; Gorini, V.; Kossakowski, A.; Sudarshan, E. C. G. J Math Phys 1976, 17, 821; Alicki, R.; Lendi, K. Quantum Dynamical Semigroups and Applications: Lecture Notes in Physics 286; Springer: New York, 1987.
5. Stewart, J. J. P. J Comput Chem 1989, 10, 209; 1989, 10, 221.

6. Choi, C. H.; Kertesz, M.; Dobrin, S.; Michl, J. Theor Chem Acc 1999, 102, 196.
7. Lee, C.; Yang, W.; Parr, R. G. Phys Rev B 1988, 37, 785; Becke, A. D. Phys Rev A 1988, 38, 3098; Miehlich, B.; Savin, A.; Stoll, H.; Preuss, H. Chem Phys Lett 1989, 157, 200.
8. Frisch, M. J., et al. Gaussian 94 (Revision C.3); Gaussian, Inc.: Pittsburgh, PA, 1995.
9. Phillips, D. L.; Zgierski, M. Z.; Myers, A. B. J Phys Chem 1993, 97, 1800.
10. Takahashi, A.; Mukamel, S. J Chem Phys 1994, 100, 2366.
11. Chen, G. H.; Mukamel, S. J Am Chem Soc 1995, 117, 4945.
12. Yokojima, S.; Chen, G. H. Chem Phys Lett 2002, 355, 400.
13. Bloch, F. Phys Rev 1946, 70, 460; Phys Rev 1957, 105, 1206.
14. Mukamel, S. Principles of Nonlinear Optical Spectroscopy; Oxford: New York, 1995.
15. Yokojima, S.; Chen, G. H. Phys Rev B 1999, 59, 7259; Chem Phys Lett 1998, 292, 379; Liang, W. Z.; Yokojima, S.; Zhou, D. H.; Chen, G. H. J Phys Chem A 2000, 104, 2445.
16. Runge, E.; Gross, E. K. U. Phys Rev Lett 1984, 52, 997.
17. Ring, P.; Schuck, P. The Nuclear Many-Body Problem; Springer: Berlin, 1980.
18. Trotter, H. F. Proc Am Math Soc 1959, 10, 545.